RF 대역통과필터 응용을 위한 FBAR 소자

윤기완, 최성창[*]

한국정보통신대학원대학교

[*]마이크로스케일 (주)

FBAR devices for RF bandpass filter applications

Giwan Yoon and Sungchang Choi[*]

Information and Communications University (ICU)

E-mail: gwyoon@icu.ac.kr

[*]MicroScale Co Ltd.

요 약

본 논문에서는 압전박막 및 이들의 FBAR 소자 응용에 대한 연구를 발표 한다. FBAR 소자는 상부 및 하부 전극 사이에 압전체가 삽입되어 있는 공진부와 SiO_2/W 이 여러층으로 적층되어 있는 음향반사층부분 크게 두 부분으로 구성되어 있다. 시뮬레이션 및 측정을 통하여 제작된 여러가지 FBAR 소자들을 평가하였다. 실험결과 우수한 삽입손실, 반사손실 및 품질계수가 얻어졌다. 따라서 FBAR 기술은 RF 대역 필터 응용을 위해서 대단히 유망한 기술로 생각된다.

ABSTRACT

In this article, piezoelectric films and their application for film bulk acoustic resonator (FBAR) devices are presented. The FBAR is composed of piezoelectric film sandwiched between top and bottom electrodes and an acoustic reflector of SiO_2/W stacked multilayers. Various FBAR devices were fabricated and evaluated through simulation and measurement. The insertion loss, return loss and Q-factor were observed to be reasonably high and good. The FBAR technology seems very promising particularly for RF band filter application.

KEYWORDS

FBAR, piezoelectric ZnO film, return loss, two-step deposition

I. Introduction

The demands for high performance filters have never been greater and become increasingly apparent as the spectrum crowding increases [1]. The so-called film bulk acoustic resonator (FBAR) devices have become one of the most promising components, mainly due to their small size, high performance and strong potential for the realization of microwave monolithic integrated circuits (MMIC) [2]. The most critical factor determining the resonance characteristics of FBAR devices is the piezoelectric property of the ZnO films, which is directly related to the degree of the preferred orientation of the ZnO crystal structure. Considerable effort has been made to fabricate high-quality ZnO films with a strongly preferred orientation. However, each approach has shown its own limitations such as the complexity of the fabrication methods and the high cost of process equipment [3]-[4]. From the manufacturing perspective, it is highly desirable to develop processes that do not deviate significantly from conventional techniques, which in this case involve the use of RF sputtering techniques for the formation of piezoelectric ZnO films, in order to retain process simplicity.

In this work, we have investigated several types of ZnO films along with several critical sputtering process parameters such as deposition pressure, RF power and O_2 concentration to clarify their impacts on the resulting crystal structures and surface morphology of the deposited films. The ZnO films formed by two-step deposition have shown a strongly preferred orientation towards the c-axis. The two-step RF sputtering deposition seems very promising and effective for fabricating high-quality ZnO films and thus suitable for FBAR applications.

II. ZnO Film Deposition and FBAR Device Fabrication

The experiment for FBAR device fabrication can be classified into two major parts as follows. The first one is the investigation of the piezoelectric ZnO films, and the other is the investigation of the FBAR devices. To study the process dependence of the ZnO films, 1200Å thick gold (Au) films were evaporated on Si (100) wafers prepared with ultrasonic precleaning in acetone and alcohol, followed by ZnO film deposition with RF sputtering under various process conditions of deposition pressure, RF power and O_2 concentration. All the films were deposited at room temperature with the substrate-to-target distance maintained at 7.6 cm. The two major interests in this work are the preferred orientation and surface roughness of the deposited ZnO films, both of which may have significant impact on the resonance property and reliability of FBAR devices. To investigate the crystal structures of the ZnO films, an X-ray diffractometer (XRD) and scanning electron microscopy (SEM) were used. In addition, atomic force microscopy (AFM) was used to measure the surface roughness of the ZnO films. To study the resonance characteristics of the FBAR devices, seven reflection layers as an acoustic Bragg reflector were formed by alternately depositing silicon dioxide (SiO_2) and tungsten (W) films. This can acoustically isolate the ZnO resonating part from the Si substrate more effectively due to the large difference in acoustic impedance between the two materials ($SiO_2 = 1.31 \times 10^7$ kg/m^{2}s, $W = 10.1 \times 10^7$ kg/m^{2}s). Then, 1200 Å thick Au films were evaporated on the top SiO_2 reflector layer and patterned by conventional photolithography to form the bottom electrodes. On the patterned Au bottom electrodes, ZnO films were deposited by two-step RF sputtering deposition. Finally, the FBAR devices were completed by evaporating and patterning 1300 Å thick aluminum (Al) films to form the top electrodes on the deposited ZnO layer. The schematic of the fabricated FBAR structure is shown in **Fig. 1**.

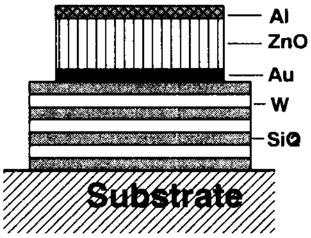

Fig. 1 Schematic of FBAR device: cross-sectional view

III. Results and Discussion

Surface morphologies of the ZnO films deposited under various deposition pressures were investigated using both SEM and AFM. For the various deposition pressures, RF power and O_2 concentration were maintained to be 120 W and 50%, respectively. Increasing the deposition pressure has resulted in larger grains. In terms of actual grain size, the low pressure of 5 mTorr has resulted in 30~40 nm grains while 120~150 nm grains were grown at 20 mTorr pressure. This is because the increase in deposition pressure also increases the number of atoms, which arrive at the film surface. In effect, the film growth rate increases, resulting in larger grains. AFM measurements were also made to investigate the surface roughness of the deposited films. The ZnO films deposited at both 5 mTorr and 10 mTorr pressures have a very similar surface roughness of ~10 Å. However, at 20 mTorr, the surface roughness increased to ~70 Å. Both SEM and AFM measurements showed that fine grain and flat surface crystals are formed at lower deposition pressures while higher deposition pressures result in larger grains and rougher surface crystals. This is believed to be mainly due to the increased deposition rate. The film deposited at 5 mTorr resulted in poor preferred orientation ZnO crystals. However, both 10 mTorr and 20 mTorr have resulted in strongly preferred orientation. The higher deposition pressure resulted in larger grains and rougher surface crystals primarily due to the increased growth rate, and a more enhanced preferred orientation is also achieved. XRD and AFM measurements were also performed on the ZnO films deposited under various RF powers. For the various RF powers, the deposition pressure and O_2 concentration were fixed 10 mTorr and 50%, respectively. Increasing the RF power was found to result in more enhanced growth toward the c-axis. The effects of various O_2/Ar ratios for ZnO deposition were investigated. For the various O_2/Ar ratios, the RF power and deposition pressure were maintained to be 120 W and 10 mTorr, respectively. The surface roughness decreased with increasing O_2. Without the use of O_2 gas (*i.e.*, in pure Ar ambient), the surface roughness was ~60 Å, whereas with 75% O_2 gas, the surface roughness was reduced to ~10 Å. More O_2 gas in the sputter chamber appears to reduce the sputter yield and hence reduce the deposition rate, mainly because of the increased collision rate between Ar and O atoms. Moreover, O_2 gas tends to increase the resistivity of the ZnO films. As compared with a 50% O_2 partial pressure, both 0% and 25% cases resulted in a significantly lower resistivity of less than 1000 Ωcm. By controlling the deposition pressure or RF power, increasing the deposition rate resulted in a ZnO film with more strongly preferred orientation toward the c-axis and it increased the surface roughness. However, by controlling the O_2 concentration, decreasing the deposition rate reduced the surface roughness. In this work, a two-step deposition technique was introduced in order to further improve ZnO film. The two-step deposition conditions are summarized in **Table I**.

Table I. ZnO Film Deposition Condition

Step	RF Power	Gas Pressure	O_2 Concentration
1	90 W	5 mTorr	75%
2	120 W	10 mTorr	50%

In the first step (step 1), the RF power, gas pressure and O_2 concentration are controlled to obtain a lower deposition rate and thus finer grains. The lower RF power and gas pressure decrease the number of Zn and O atoms on the Au electrode, eventually allowing each atom to find more suitable sites. The higher O_2 concentration appears to enhance the formation of finer grains. First, the initial 0.1 μm thick ZnO film was deposited in step 1, then followed by the step 2 deposition. Between the two steps, the deposition condition was immediately changed in order to increase the film deposition rate in step 2. As a result, the initial 0.1 μm thick film with fine grains was deposited on the amorphous Au electrode with a low deposition rate. Then, strongly preferred columnar grains were grown with a high growth rate, eventually resulting in fine columnar grain structures. The ZnO films deposited by the two-step deposition technique were compared with those deposited by the conventional deposition technique, as shown in **Fig. 2**.

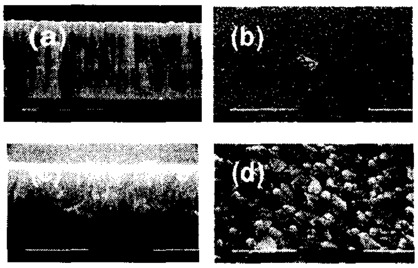

Fig. 2 SEM of ZnO films deposited by two-step and conventional techniques.

The ZnO films deposited by the two-step deposition technique were compared with those deposited by the conventional deposition technique. Conventional deposition resulted in random crystal grain structures [**Fig. 2(c)**] and large grains (~500 nm) [**Fig. 2(d)**], whereas two-step deposition resulted in ZnO films with more strongly preferred orientation towards the c-axis [**Fig. 2(a)**] and relatively fine grains (~50 nm) [**Fig. 2(b)**]. One-port FBAR devices were fabricated and measured for the S-parameter extraction. An HP 8510 network analyzer and a Cascade Microtech probe station were used for FBAR measurements. Prior to the FBAR measurement, the RF probing system was accurately calibrated using the cascade calibration substrate. The one-port FBAR devices with the resonance area of 150 μm x 150 μm were measured using the G-S-G probe. For the S-parameter measurement, the RF signal was applied to the bottom electrode through one signal contact (S) and top electrode through two ground contacts (G). A large return loss of ~35 dB was achieved at center frequency of ~1.95 GHz [**Fig. 3**].

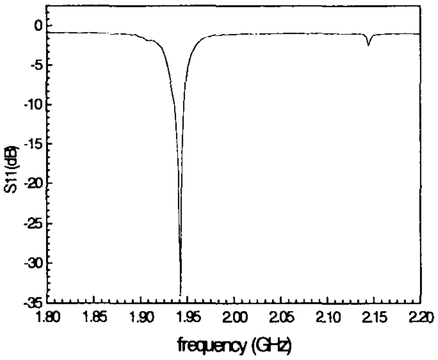

Fig. 3 Return loss (S_{11}) of FBAR device

The resonance behavior of the FBAR device exhibits its characteristic impedance as a loop that is mostly located in the capacitive part on the Smith chart, as plotted in **Fig. 4**.

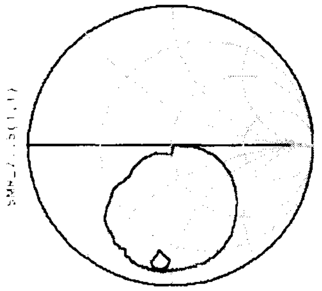

Fig. 4 Smith chart of the FBAR device

The Smith chart shows that the FBAR is already matched to 50Ω impedance without any outer matching circuits. This implies that the FBAR device could be easily matched by simply adjusting its resonance area. The area matched well to 50Ω impedance was found 150 μm x 150 μm. The seven layers reflector shows a relatively large return loss of almost 35 dB. In general, two different definitions have been used to find fs and fp. One is the conventional definition of using the local extrema in the magnitude of the input impedance (Z_{in}). The other is the empirical definition of using the local extrema in the slope of the input impedance phase (Z_{in}). In this work, the empirical definition was used to calculate fs and fp from the slope of Z_{in} vs. frequency plot [**Fig. 5**].

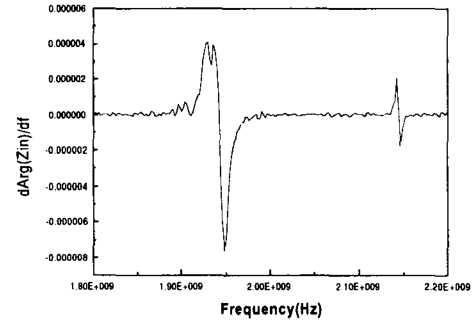

Fig. 5 Slope of input impedance vs. frequency plot

As a result, a high Q factor of ~4000 was obtained.

IV. Conclusion

A two-step deposition was investigated to attain high-quality ZnO films for the FBAR applications. In addition, the characteristics of the FBAR devices were also investigated, which was found to be closely related to the multi-layer reflector. The seven layers reflector showed a large return loss of ~35 dB, leading to a high Q factor of about 4000. This FBAR technology seems very promising for RF filter applications.

References

[1] K. M. Lakin, G. R. Kline and K. T. McCarron : IEEE Trans. Microwave Theory & Tech. **43** (1995) 2933.

[2] S. V. Krishnaswamy, J. F. Rosenbaum,

S.Howitz and R. A. Moore: IEEE Ultrasonics Symp. (1990) p. 529.

[3] J. C. Zesch, B. Hadimioglu, B. T. Khuri-Yakub, M. Lim, R. Lujan, J. Ho, S.Akamine, D. Steinmetz, C. F. Quate and E. G. Rawson: IEEE Ultrasonics Symp. (1991) p. 445.

[4] M. Kadota, T. Kasanami and M. Minakata: IEEE Trans. Ultrason. Ferroelectr. & Freq. Control **41** (1994) 479.